JOURNAL OF CATALYSIS 84, 74–84 (1983)

Catalytic Properties of Defective Brannerite-Type Vanadates

III. Oxidation of *o*-xylene on $Mn_{1-x}\phi_xV_{2-2x}Mo_{2x}O_6$

JACEK ZIÓŁKOWSKI[1] AND MARIAN GĄSIOR

Institute of Catalysis and Surface Chemistry, Polish Academy of Sciences, ul. Niezapominajek, 30-239 Kraków, Poland

Received May 27, 1982; revised January 12, 1983

Part I of this series (J. Catal. 81, 298 (1983)) described the catalytic anisotropy of $Mn_{1-x}\phi_xV_{2-2x}Mo_{2x}O_6$ solid solutions in the oxidation of propylene. In Part II (J. Catal. 81, 311 (1983) a new model of sites active in oxidation reactions has been proposed to explain this phenomenon. This model, designated BSMAS, is based on crystallochemical considerations and on the assumption that the individual catalytic activity of a given surface oxygen atom is proportional to its reciprocal bond-strength sum. In this paper the studies are extended to the oxidation of *o*-xylene. The conversion and yield of phthalic anhydride, tolualdehyde, phthalide, maleic anhydride, CO, and CO_2 have been determined as a function of temperature, contact time, catalyst composition, and type of preferentially exposed crystallographic plane ((201) or (20$\bar{2}$)). It is shown that the reaction scheme is composed of "one-stage" total combustion and of a one-site "rake-reaction" along which C_8 products are formed. The scheme is common for both planes and it does not alter with catalyst composition, but, as is shown by results from changes of conversion, yields, and selectivities to different products, the rate constant of the elementary steps does depend on the plane exposed and on the composition of the solid. Discussion in terms of the BSMAS model makes it possible to indicate the structure of active sites on which the abovementioned reactions may take place and to explain the plane effect and the dependence of the reaction pattern on catalyst composition.

INTRODUCTION

Part I of this series (*1*) describes the catalytic anisotropy of $Mn_{1-x}\phi_xV_{2-2x}Mo_{2x}O_6$ ($0 \leq x \leq 0.45$) solid solutions in the oxidation of propylene. It is useful to recall some details which are directly related to the subject matter of the present paper.

The solutions $Mn_{1-x}\phi_xV_{2-2x}Mo_{2x}O_6$ (further denoted as MV-*X*, where $X = 100x$) are of monoclinic, *C*2/*m*, brannerite-type structure. They were prepared by solid state synthesis (*1, 2*) starting from the respective mixtures of Mn_2O_3, V_2O_5, and MoO_3. Depending on the conditions of the final thermal treatment the shape of the grains of powder sample changed and the (201) plane or the (20$\bar{2}$) plane prevailed in their external surface. When pressed in the X-ray sample holder the laminar grains oriented and this brought about a strong change in the intensity *I* of the reflections corresponding to the above planes. A morphological factor defined as $f = I_{201}/I_{20\bar{2}}$ was taken as a semiquantitative measure of the contribution of the two planes in the external surface of the grains. The theoretical value of $I_{201}/I_{20\bar{2}}$, nearly independent of composition, equals 1.13–1.16. For the purpose of catalytic studies two series of preparations were selected. The first, labeled MV-X-(201), comprised samples with *f* values between 1.8 and 2.0, thus exposing preferentially the (201) plane. The second series, labeled MV-X-(20$\bar{2}$), included samples with $f = 1.2$–1.4, the contribution of the two planes under discussion being thus comparable in this series. However, due to the much higher catalytic activity of the (20$\bar{2}$) plane as compared to the (201) the

[1] To whom correspondence should be addressed.

0021-9517/83 $3.00

results obtained for MV-X-(20$\bar{2}$) may be regarded as sufficiently representative for the (20$\bar{2}$) plane only.

Oxidation of propylene over MV-X yielded six products: acrolein, acrylic acid, acetaldehyde, acetic acid, CO, and CO_2. It has been found that the (201) plane is much less active and the yield vs contact time curves have shown that more and more oxidized products (aldehydes, acids, CO, CO_2) appear in the sequence characteristic for consecutive reactions. This proves that on the (201) plane predominate the active sites capable of successive, one by one, incorporation of oxygen atoms into the molecule of propylene, separated by the desorption and adsorption processes. On the contrary, samples exposing the (20$\bar{2}$) plane are more active and the initial selectivities towards all six quoted products have reached measurable values. This suggests that the (20$\bar{2}$) plane is characterized by active sites able to incorporate, without desorption, more than one oxygen atom to the molecule of propylene. The common feature of both planes is that the total combustion drastically diminishes with the increase of the composition parameter x.

To explain the abovementioned catalytic features a new model of active sites has been developed in Part II (*3*). It has been assumed that the mechanism of transformation of π-allyl (which is the first intermediate species of propylene oxidation) depends on the number and configuration of active, surface oxygen atoms around the adsorption site. Structural considerations have been based on crystallographic data and the individual activities of surface oxygen atoms have been assumed to be proportional to the reciprocal sums of the strength of bonds to them (Σs_i) from the adjacent cations, calculated according to the bond length–bond strength concept (*4*). In particular, surface oxygen atoms of $\Sigma s_i \approx 2$ are regarded as inactive and those of $\Sigma s_i < 1.85$ as active in catalytic oxidation of hydrocarbons. As a rule, the crystal is "cut" in such a manner as to conserve the stoichiometric composition. Oxygen atoms completing the polyhedra around the cations are regarded as adsorbed atoms. Their Σs_i values are less than 1. Only a fraction of such sites is occupied by adsorbed oxygen. All possible interactions between propylene (or π-allyl) adsorbed over Mn, V, or Mo positions of (201) and (20$\bar{2}$) planes with the neighboring active oxygens were analyzed. The analysis enabled us to indicate the probability of appearance of different reaction products as a function of composition and kind of the exposed crystallographic plane. The results of this analysis are well consistent with the experimental facts (*1*). The abovementioned bond strength model of active sites designated (BSMAS) has also been successfully applied to explain the catalytic anisotropy of MoO_3/graphite catalysts in the oxidation of propylene (*5*).

It seemed of interest to check if the effect of anisotropy may also be observed in the oxidation of a molecule as large as *o*-xylene (OX). One may expect that the OX molecule would be adsorbed in the plane parallel to the surface and form a π-complex with a coordinately unsaturated surface metal atom. On this assumption the BSMAS model may be applied. As we deal with a molecule large in comparison with propylene, it might interact with active oxygens adjacent to the adsorption site as well as with more distant atoms. Due to this fact the catalytic properties of different active sites on different planes might be rendered uniform.

EXPERIMENTAL

Catalytic studies involved two series of preparations: MV-X-(201) [comprising MV-0-(201), MV-15-(201), MV-25-(201), and MV-30-(201)] and MV-X-(20$\bar{2}$) [comprising MV-0-(20$\bar{2}$), MV-10-(20$\bar{2}$), MV-15-(20$\bar{2}$), and MV-30-(20$\bar{2}$)]. The quoted samples come from the same batches as used in Part I (*1*), except for MV-25-(201) which was prepared in an analogous way. Their main characteristics have already been described

in the Introduction and details are given elsewhere (*1, 2, 6*). The X-ray and DTA patterns of the catalysts were the same before and after catalytic experiments, which proves that in the limit of sensitivity of the applied methods the samples were not altered during catalytic reactions.

To characterize the surface structure of the MV-X solid solutions XPS studies were undertaken with a Vacuum Generators ESCA-3 spectrometer. The Au $4f_{7/2}$ line at 84.0 eV was taken as a reference. Experiments were performed for three samples of different composition after treatment *in situ* by heating the sample at 100°C and 10^{-7} Torr for 1 h ("fresh sample") or at 500°C and 10^{-8} Torr for 10 h ("reduced sample"). In both cases O 1*s*, V 2*p*, Mo $3d_{3/2}$, and Mn 2*p* lines appeared at 530.3, 517.0, 232.6, and 641.3 eV (±0.2 eV), respectively, proving that the samples are resistant to thermal treatment and reduction. The quoted values of binding energy are typical for O^{2-}; V^{5+}, and Mo^{6+} ions (*7–9*). Only that for Mn 2*p* is slightly increased (literature data are 640.6 eV for MnO and 641.4 eV for Mn_3O_4 (*9*)), which may be ascribed to the bond polarization effect. Preliminary analysis of the line intensities suggests that on "reduction" the surface becomes slightly enriched in vanadium. However, no effects were observed which could indicate segregation of any new phase on the surface.

Catalytic testing was performed in a flow reactor, operating at atmospheric pressure, at 370–470°C. The catalyst volume was 2 ml diluted with 4 ml of glass, the grain size of both components being 0.5–1.0 mm. The feed gas contained 44 g of OX per 1 m^3 of air and its flow rate was 30 liters/h in the standard tests and varied between 15 and 120 liters/h in the kinetic experiments. Contact time was calculated as catalyst volume divided by volume flow rate of the feed gas. At a given temperature the reaction was carried out until a constant value of the yield of products was obtained. The reactor was directly connected to a gas chromatograph (Chromatron G.Ch.F. 18.4) by means of a system of heated six-way valves. Phthalic anhydride (PA), tolualdehyde (TA), phthalide (Ph), *o*-toluic acid (appearing in trace amounts), maleic anhydride (MA), and unreacted OX were analyzed on a 2 m × 4 mm column filled with 5% F-50 oil on Chromosorb G 80/100 kept at 180°C, with a N_2 flow rate of 25 ml/min. Total oxidation products were analyzed using a 2 m × 4 mm column with Chromosorb 104 (for CO_2) and a 1-m-long column with molecular

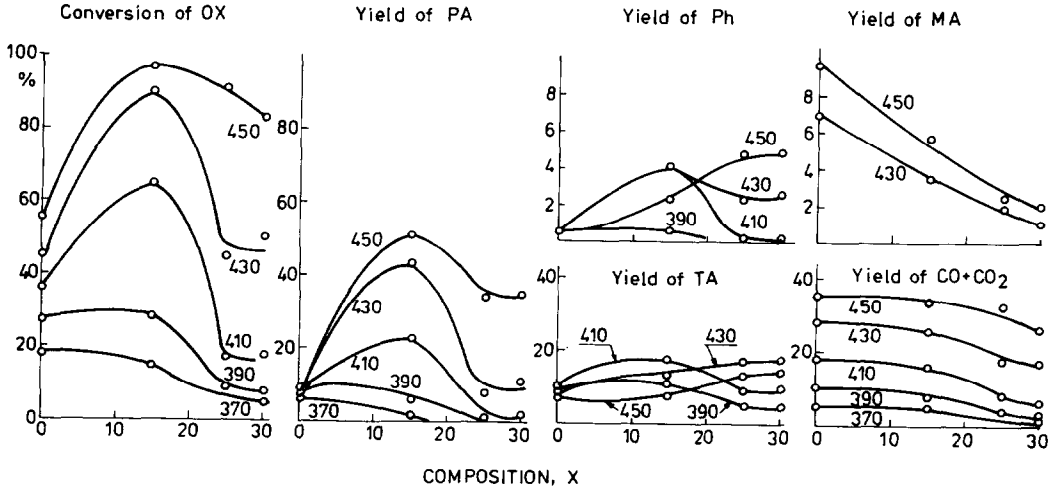

FIG. 1. Conversion of OX and yields of PA, TA, C_1, Ph, and MA on MV-X-(201) as a function of catalyst composition and temperature.

sieves 13X (for CO). The total carbon balance was higher than 95%.

RESULTS AND DISCUSSION

Figures 1 and 2 summarize the results obtained in conversion-composition and yield-composition coordinates as measured at 370–450°C for the MV-X-(201) and MV-X-(20$\bar{2}$) series, respectively. Selectivities towards the main reaction products for representative samples are calculated and presented in Fig. 3 as a function of reaction temperature and in Fig. 4 as a function of conversion.

As can be seen from Figs. 1 and 2, MV-0-(20$\bar{2}$) is the most active of all the samples studied. Already at 390°C a conversion of 75% is observed whereas conversion does not exceed 25% for all other samples of both series at this temperature. Activity (conversion) decreases monotonically along the MV-X-(20$\bar{2}$) series. MV-0-(20$\bar{1}$) is roughly half as active as MV-0-(20$\bar{2}$) and conversion passes through a maximum along the MV-X-(201) series. The maximum observed for MV-15-(201) is so distinct that the conversion-temperature dependences for the MV-15 samples of both series (which may be easily deduced from the data shown in Figs. 1 and 2) nearly overlap.

The common feature of all the catalysts is a relatively high (25–45%) selectivity to C_1(CO + CO_2) products at low temperatures (370°C) and low conversions (~10%). As this selectivity usually diminishes with increasing temperature and conversion (at least for Mo-doped samples), it cannot be ascribed to the consecutive combustion of C_8 products. This suggests that on both planes of MV-X active sites are present which initiate the total degradation of the o-xylene (OX) molecule in "one stage." One may imagine that these sites are surrounded by several active oxygen atoms which cause the breakage of the OX molecule, and in particular its aromatic ring, into several unsaturated, partly oxidized, and highly reactive radicals. These radicals may be transformed to CO and CO_2 already on the catalyst surface (moving along it and reacting with active surface oxygen atoms) or after desorption in rapid homogeneous reactions.

At the highest temperatures and conversions the Mo-doped samples of both series usually show a small increase of selectivity to C_1 at the expense of that to C_8. This indicates the consecutive combustion (at low

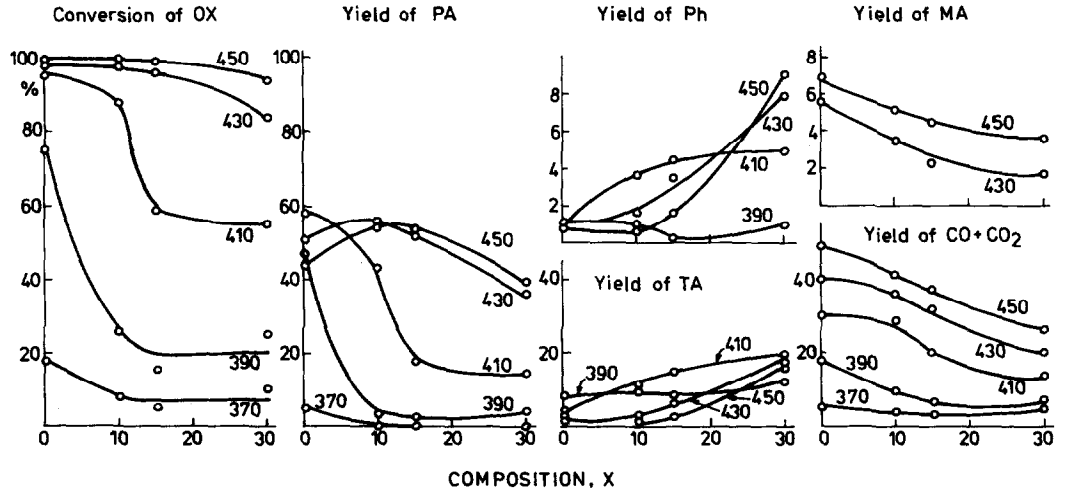

FIG. 2. Conversion of OX and yields of PA, TA, C_1, Ph, and MA on MV-X-(20$\bar{2}$) as a function of catalyst composition and temperature.

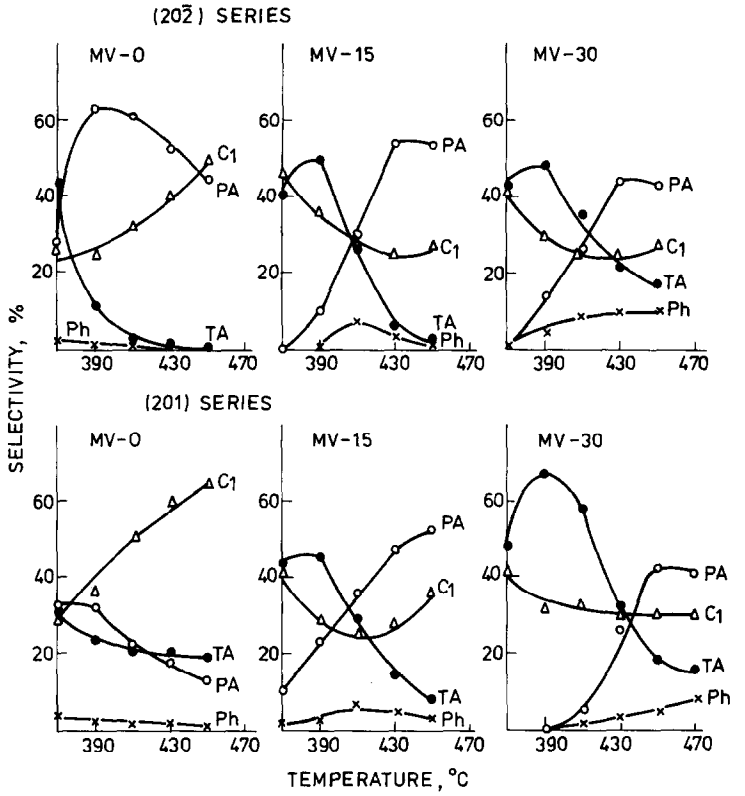

FIG. 3. Selectivities to the main reaction products on the catalysts of the MV-X-(201) and MV-X-(20$\bar{2}$) series as a function of temperature.

efficiency) of preformed C_8 products, which might proceed on the same active sites as those on which "one-stage" degradation takes place. This last process is much more efficient for the MV-0 samples of both series, especially for MV-0-(201), and masks the route to C_8 products so much that the pathway is better deduced from the data obtained for the Mo-doped samples than for the Mo-free samples.

Thus, for the partial oxidation products, TA (whose yield and selectivity pass through maxima) is the main reaction product at low temperatures and low conversions, whereas at higher temperatures and conversions the dominating product becomes PA. The selectivities and yields of Ph pass through a maximum or show such a tendency. These facts suggest that TA, Ph (probably), and PA are formed via consecutive reactions.

On the other hand, if one omits the narrow reaction onset range (350–390°C), the selectivity-temperature and the selectivity-conversion curves (Figs. 3 and 4) clearly demonstrate that TA and PA appear alternatively. This suggests that C_8 products are formed according to the "rake mechanism." The increasing temperature should favor the abstraction of oxygen from the lattice and desorption of preadsorbed species in a more oxidized form (PA). It is interesting to note that the last component reaction of the rake (combustion) would be of minor efficiency (for Mo-doped samples) in spite of the fact that very "aggressive" sites ("one-stage" combustion) are present on the surface. Consequently one has to assume that the rake mechanism is effected on one site which should be surrounded by three active oxygen atoms necessary for PA formation. Similarly to the oxidation of

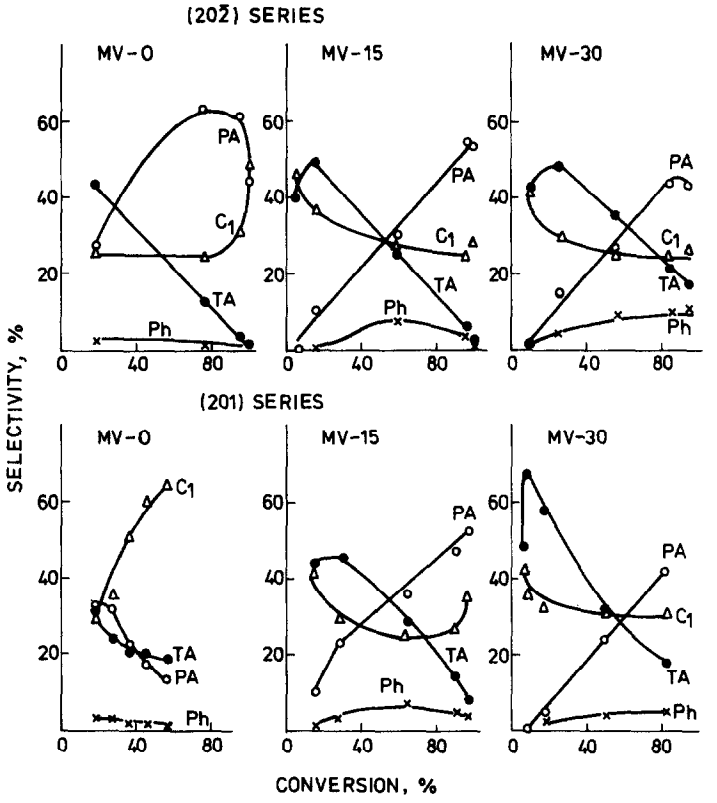

FIG. 4. Selectivities to the main reaction products on the catalysts of the MV-X-(201) and MV-X-(20$\bar{2}$) series as a function of conversion.

propylene (*1, 3*) it is assumed that the abstracted hydrogen atoms may move along the surface and combine with distant loosely bound oxygen to form H_2O.

To decide if C_8 products are formed with a consecutive mechanism or the rake mechanism, yield–contact time dependences were determined. The results are presented in Fig. 5 and show that (at least at short contact time) the products of partial oxidation are formed by seemingly parallel reactions, thus confirming the rake mechanism. The yield of C_1 products is already high at short contact time and slightly dependent on its further increase. This suggests that "one-stage" total combustion proceeds at high and constant coverage of the respective sites and that this reaction pathway is rate-determined by surface reaction or by desorption of products. This also suggests, once again, that C_1 and C_8 products are formed on different active sites.

As follows from the above discussion, oxidation of *o*-xylene proceeds on (201) and (20$\bar{2}$) planes of MV-X solid solutions with the same mechanism. It is initiated on two different active sites, one of them being responsible for "one-stage" total combustion and the other for the selective formation of C_8 products by a one-site rake mechanism. The C_8 products preformed are consecutively combusted, the efficiency of this process being dependent on catalyst composition. However, although the reaction scheme is common for both planes under discussion and all samples of various composition, the rate constant of the elementary steps must be differentiated. The yield, and especially the distribution of products for Mo-doped samples are nearly plane in-

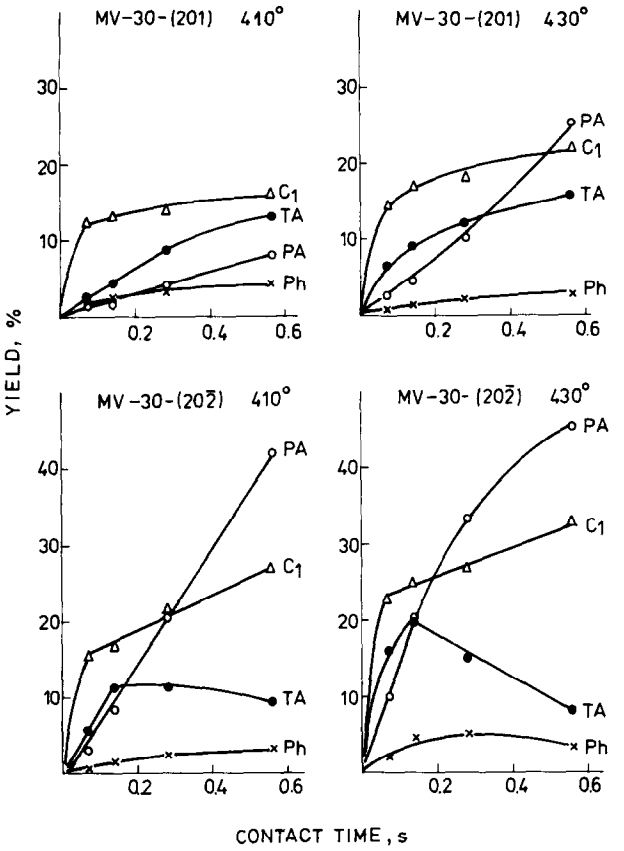

FIG. 5. Yield of the main reaction products on MV-30-(201) and MV-30-(202) at 410 and 430°C as a function of contact time.

dependent, the (20$\bar{2}$) plane being slightly more active. On the other hand, the (201) and (20$\bar{2}$) planes of the MV-0 sample differ markedly. The (20$\bar{2}$) plane is roughly twice as active as the (201) plane and yields quite a large amount of C_8 product. The best results, obtained for MV-0-(20$\bar{2}$) at 410°C, are 95% conversion, 58% PA, 8% TA, 30% C_1. By contrast, the highest conversion for MV-0-(201) amounts at 450°C to 56% but CO and CO_2 (49% together) are the main reaction products. The yields of TA and PA are never higher than 10%, showing the nonselectivity of this plane in the partial oxidation.

APPLICATION OF THE BOND-STRENGTH MODEL OF ACTIVE SITES (BSMAS)

The principle of the BSMAS in the reactions of oxidation of hydrocarbons has been explained in the Introduction and the details are given in previous papers (*3*, *5*). Figures 6 and 7 show the arrangement of atoms on the (20$\bar{2}$) and (201) planes of MnV_2O_6, respectively. As for the vertical coordinates see Part II (*3*) and Figs. 8 and 9 in which the side views are shown. In the interior of the brannerite-type structure there are three nonequivalent oxygen atoms of different, threefold coordination: O_1(V, Mn, Mn), O_2(V, V, Mn), and O_3(V, V, V). Knowing the respective metal–oxygen distances one may easily calculate the respective s_i and Σs_i values, as described in Part II (*3*). On the surface some bonds are "cut out" and due to this fact the number of oxygens which are nonequivalent from the point of view of coordination and bond-

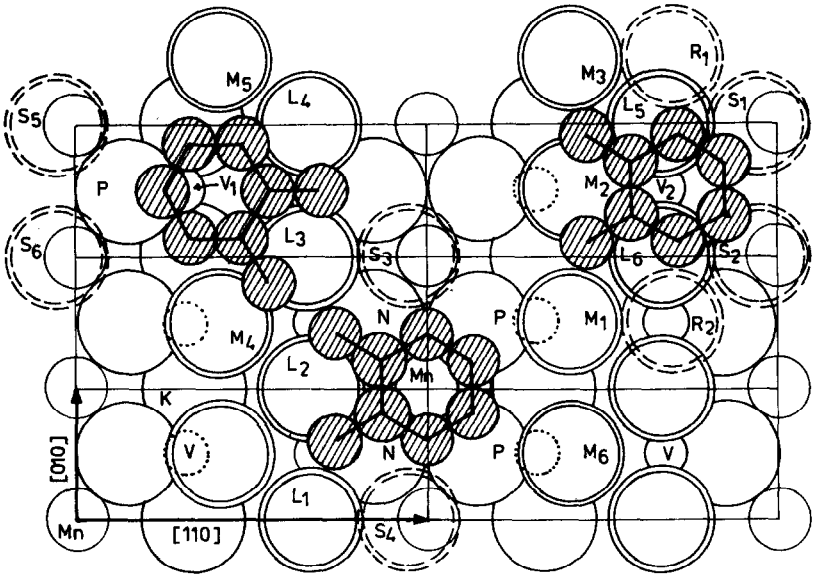

FIG. 6. o-Xylene (dashed circles) adsorbed on three different sites on the (20$\bar{1}$) plane of MV-X. Small circles—vanadium, medium circles—manganese, large circles—oxygen, large dashed circles—adsorbed oxygen, large double circles—active oxygen, dotted circles—some covered atoms.

ing increases. They are labeled with different capital letters. Further differentiation of oxygens takes place on doping with molybdenum as some bonds disappear (due to the formation of cation vacancies in the original Mn sites) and the length and nature of others is altered (due to the substitution of Mo for V). As an example we may indicate a bulk O_2(V, V, Mn) atom; when exposed on the (201) plane of MnV_2O_6 it loses one of its V neighbors and becomes O_F(–, V, Mn); on doping its neighborhood may be changed

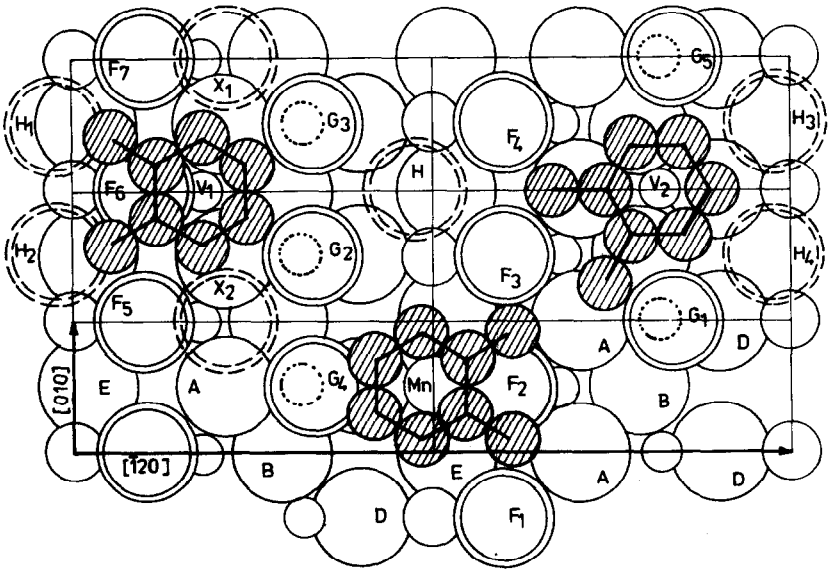

FIG. 7. o-Xylene adsorbed on three different sites on the (201) plane of MV-X (cf. Fig. 6).

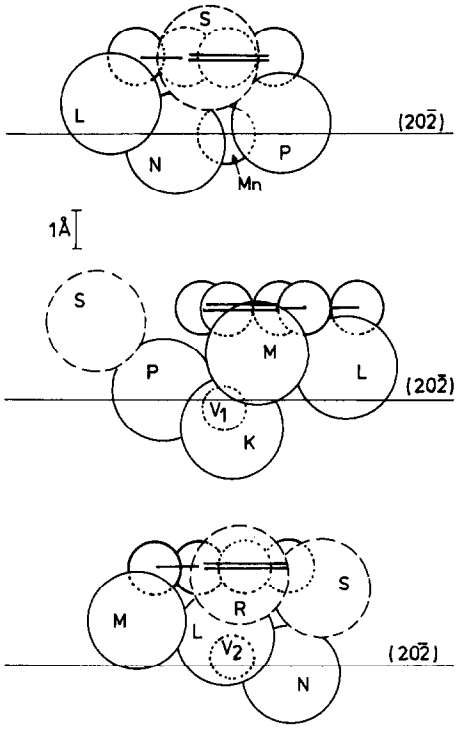

FIG. 8. Side views of *o*-xylene adsorbed on three different sites of the (20$\bar{2}$) plane of MV-X (cf. Fig. 6).

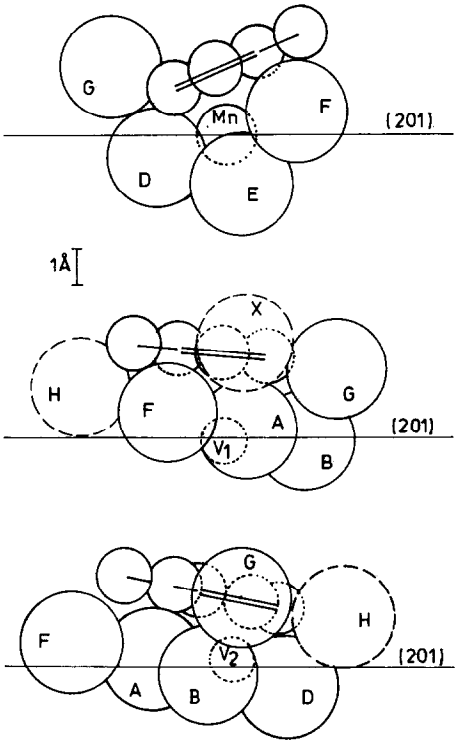

FIG. 9. Side views of *o*-xylene adsorbed on three different sites of the (201) plane of MV-X (cf. Fig. 7).

to O_F(–, V, ϕ), O_F(–, Mo, Mn), or O_F(–, Mo, ϕ), where ϕ indicates a vacancy. These changes are followed by the respective modifications of Σs_i values. Some Σs_i values of active surface oxygen atoms originally calculated in Part II (*3*) and directly related to the present discussion are recalled in Table 1.

As already mentioned, the OX molecule is expected to be adsorbed as a π-complex

TABLE 1

Σs_i Values for Active Surface Oxygen Atoms (*3*)

Oxygen	(201) plane coordination	Σs_i	Oxygen	(20$\bar{2}$) plane coordination	Σs_i
O_G	(V, –, –)	1.42	O_L	(V, V, –)	1.68
O_G	(Mo, –, –)	1.65	O_L	(V, Mo, –)	1.75
			O_L	(Mo, Mo, –)	1.81
O_F	(–, V, Mn)	1.84	O_M	(V, V, –)	1.58
O_F	(–, V, ϕ)	1.45	O_M	(V, Mo, –)	1.55
O_F	(–, Mo, Mn)	2.07	O_M	(Mo, V, –)	1.81
O_F	(–, Mo, ϕ)	1.68	O_M	(Mo, Mo, –)	1.79
O_H	(–, Mn, Mn)	0.50	O_S	(–, –, Mn)	0.39
O_X	(V, –, –)	0.13	O_R	(V, –, –)	0.43
O_X	(Mo, –, –)	0.11	O_R	(Mo, –, –)	0.42

over coordinately unsaturated surface metal atoms. Numerous orientations of adsorbed OX may be imagined. The present discussion will involve a limited number of them, namely, the orientations for which the interactions between OX and surface oxygens seem to be the most efficient from the catalytic viewpoint. The chosen examples are visualized in Figs. 6 and 7 and their side views are shown in Figs. 8 and 9. The steric possibilities and hindrances resulting from the dimensions of atoms and their spatial distribution were taken into account in constructing the figures. For simplicity, the hydrogen atoms of OX are omitted and the inclination of OX to the surface (cf. Fig. 9) is neglected in Fig. 7.

As follows from Figs. 6 and 7 the OX molecule adsorbed on each of six different sites is surrounded by several active oxygen atoms. According to their localization they may be divided into two groups: (1) oxygen atoms which may attack the alkyl groups, and (2) oxygen atoms which may attack the aromatic ring.

It is striking that at each site linear or angular triads of oxygen may be distinguished: $Mn(20\bar{2})L_1L_2L_3$, $V_1(20\bar{2})L_3L_4M_4$, $V_2(20\bar{2})M_1M_2M_3$, $Mn(201)F_1F_2F_3$, $V_1(201)F_5F_6F_7$ and $V_2(201)F_3F_4G_1$ which are localized around the alkyl groups of OX. These centers may constitute the active sites on which C_8 products are selectively formed with the one-site rake mechanism, provided that the aromatic ring of OX is not attacked and destroyed at the same time by other active oxygen atoms. If such oxygens were absent the situation would be unequivocal. At present, however, it is difficult to judge to what extent the probability of the breakage of the aromatic ring depends on the distance between the ring and the active surface oxygen, on the angular relations, and on the number of active oxygens around the ring. The conclusions, based to some extent on intuition, are summarized in Table 2.

It is also interesting to analyze the possible changes in activity and selectivity which, in the light of BSMAS, should take place on doping. Let us remark that the selective formation of C_8 products on the $(20\bar{2})$ plane depends on the activity of O_L and O_M. As follows from Table 1, with increasing x, O_L(V, V, –) and O_M(V, V, –) are successively replaced by atoms of (V, Mo, –), (Mo, V, –), or (Mo, Mo, –) coordination of higher Σs_i, and thus of lower activity. The yield of C_8 should thus decrease with x and the yield ratio of less oxidized TA and more oxidized PA should increase. These conclusions are in agreement with the experimental findings (cf. Fig. 2).

The selective formation of C_8 products on the (201) plane depends mainly on the activity of O_F and to some extent on O_G. On doping O_G(V, –, –) is replaced by the less active O_G(Mo, –, –) (Table 2). As for O_F, the situation is more complicated. Taking into account the oxygen population-composition dependences discussed in detail in Part II (*3*), we may expect that at lower x the slightly active O_F(–, V, Mn) will be replaced by the highly active O_F(–, V, ϕ) but at higher x moderately active O_F(–, Mo, ϕ) should predominate. The average activity should thus pass through a maximum, the position of which is difficult to indicate theoretically. The experimental facts (Fig. 1), however, clearly demonstrate that this happens at $x \approx 0.15$.

As can be seen from Table 2 the oxygen atoms which contribute to the breakage of the aromatic ring may be divided into three groups: (1) adsorbed over V oxygen atoms O_X and O_R, (2) adsorbed over Mn oxygens O_H and O_S, and (3) lattice oxygens O_L, O_G, and O_F. The activity of the first group is practically independent of x; the average activity of the second group diminishes with x due to the decreasing coverage (oxygen cannot be adsorbed on the cationic vacancy); the changes of the activity of the third group have already been discussed above. The resultant of the above changes seems to consist of a decrease of the probability of molecule degradation with an increase of the concentration of dopant. This

TABLE 2

Structure and Yield of Active Sites on the $(20\bar{2})$ and (201) Planes of MV-X

Site	Active oxygen atoms attacking the alkyl groups	Active oxygen atoms which eventually may attack the aromatic ring	Main products expected for MV-O	Changes in product distribution expected with increasing X
Mn $(20\bar{2})$	L_1, L_2, L_3	M_1, M_6 Very distant from the ring S_3, S_4 Close to the ring, but the expected coverage with adsorbed oxygen is small	C_8	Decrease of the yield of C_8 and of the PA/TA ratio
V_1 $(20\bar{2})$	L_4, L_3, M_4	M_5 Distant from the ring S_5, S_6 Very distant from the ring	C_8	
V_2 $(20\bar{2})$	M_1, M_2, M_3	L_5, L_6 Very close to the ring S_1, S_2 Very close to the ring R_1, R_2 Close to the ring	C_1	Decrease of the yield of C_1
V_1 (201)	F_5, F_6, F_7	G_2, G_3 Close to the ring F_6 Very close to the ring X_1, X_2 Probably may attack the ring	C_1	Decrease of the yield of C_1
V_2 (201)	F_4, F_3, G_1	G_1, G_5 Distant from the ring H_3, H_4 Distant from the ring	C_8	1. Yield of C_8 and PA/TA ratio pass over maximum
Mn (201)	F_1, F_2, F_3	G_4 Very close to the ring F_2 May attack either the ring or the alkyl groups Attack of only one active oxygen seems to be insufficient to break the ring	C_1 or C_8	2. Decrease of the yield of C_1

conclusion agrees also with the experimental facts.

It should be added that, on doping, the activities of some of the O_P, O_L, O_D, and O_E atoms also increase (*3*), and these atoms theoretically might participate in the breakage of the aromatic ring giving rise to the yield of C_1 products growing with x. Disagreement of this conclusion with experimental data suggests that these oxygen atoms, relatively deeply immersed in the bulk of crystal (as opposed to the adsorbed O_R, O_S, O_H, and O_X), have no electrophilic character, required for degradation of the aromatic ring.

ACKNOWLEDGMENTS

The authors are very grateful to Dr. Barbara Grzybowska-Świerkosz for valuable comments. We are also indebted to Dr. Jerzy Stoch and to Mr. Tomasz Czeppe for the preliminary XPS experiments.

REFERENCES

1. Ziółkowski, J., and Janas, J., *J. Catal.* **81,** 298 (1983).
2. Kozłowski, R., Ziółkowski, J., Mocała, K., and Haber, J., *J. Solid State Chem.* **35,** 1 (1980), *erratum: J. Solid State Chem.*, **38,** 138 (1981).
3. Ziółkowski, J., *J. Catal.* **81,** 311 (1983).
4. Brown, I. D., and Kang Kun Wu, *Acta Crystallogr. Sect. B* **32,** 1957 (1976).
5. Ziółkowski, J., *J. Catal.* **80,** 263 (1983).
6. Ziółkowski, J., Kozłowski, R., Mocała, K., and Haber, J., *J. Solid State Chem.* **35,** 297 (1980).
7. Sawatzky, G. A., and Antonides, E., *J. Phys. Colloq.* **C4,** *suppl.* 10, **37,** 117 (1976).
8. Haber, J., Machej, T., Ungier, L., and Ziólkowski, J., *J. Solid State Chem.* **25,** 207 (1978).
9. Oku, M., Hirokawa, K., and Ikeda, S., *J. Electron Spectrosc. Relat. Phenom.* **7,** 465 (1975).